geoconvention
Calgary • Canada • May 12-14 2025

# Investigating the shallow structure along the Denali fault using passive seismic HVSR measurements: an investigation into geothermal potential and environmental conditions

*Daniel Afolabi[1], Hersh Gilbert[1], Jan Dettmer[2], and Jeremy M. Gosselin[3]*

*[1]Dept. of Earth, Energy, and Environment, University of Calgary*

*[2]Yukon Geological Survey*

*[3]Natural Resources Canada*

## Introduction

Geothermal energy relies on heat sources and the permeability of fractured rocks for fluid circulation to transport heat to the surface. Understanding fault structures and stress regimes is crucial for resource assessment (Faulds and Hinz, 2015; Fraser et al., 2018) and can be explored using passive seismic observations (Cheng et al., 2021). Geothermal energy is a renewable energy source with less environmental impact than conventional fossil fuels. As the world transitions from non–renewable sources of energy, the Yukon Government recognizes the need to transition away from fossil fuels. To aid in identifying alternative sources of energy, the Yukon Geological Survey (YGS) is seeking to characterize zones of increased geothermal potential. Dispersed hot springs and a sparse pattern of volcanism during the Pleistocene and Holocene reveals a limited distribution of elevated geothermal potential (Russell et al. 2023).

Further studies showed that the shallowest Curie point depths of 13–15 km in the area are situated around the Eastern Denali fault near Burwash Landing (Li et al., 2017; Witter et al., 2018). Furthermore, elevated values for the crustal geotherm were estimated to reach 45°C/km (Witter, 2020). The Denali Fault around Burwash Landing was identified to possess three sub-parallel strands, highlighting its complexity and suggesting a structurally favorable environment comprised of permeable formations (Witter et al. 2018; Witter, 2020). Taken together, this evidence suggests value in further evaluating the geothermal potential in southwest Yukon.

Detailed information about the orientation and subsurface structure of the Denali Fault are limited near Burwash Landing (Witter et al., 2018; Witter, 2020). Additionally, constraints on sediment thickness have also been lacking. This provides a necessary context for determining depth to the top of the basement in the area and structural features in the near subsurface that could promote the effectual migration of geothermal fluids. This is because of the relationship between overburden thickness and geothermal resource potential. Sediments have lower thermal conductivity compared to crystalline basement rocks; hence, they are able to trap heat more effectively (Koteas et al., 2011; Balkan et al., 2017). Also, thick sediment layers act as an insulating blanket, reducing heat loss to the surface and allowing subsurface temperatures to remain higher (Koteas et al., 2011). Thick sediment cover especially one of low conductivity could also be disadvantageous as it could cause dispersion of fluids within them, making it daunting and challenging to locate their flow (Kämmlein et al., 2019). Therefore, it is important to determine the thickness of sediments overlying the basement rock as it further aids the interpretation of other data types in geothermal assessment. This is achievable by determining the fundamental resonance frequency ($f_0$) from horizontal and vertical spectral ratio (HVSR) measurements.

Seismic data for this project were acquired between June and August, 2022 using 5 Hz geophones across 34 stations (Figure 1). Horizontal-to-vertical spectral ratio (HVSR) measurements of ambient seismic noise were used to estimate the fundamental resonance frequencies of ambient noise, providing insights into the shallow velocity structure. The HVSR measurements were further correlated with meteorological data to highlight the effects of environmental factors on seismic measurements and highlight HVSR signatures that are due to structural changes rather than effect of the environment. These results were thereafter interpreted to relate to the thickness of the sediment beneath each station.

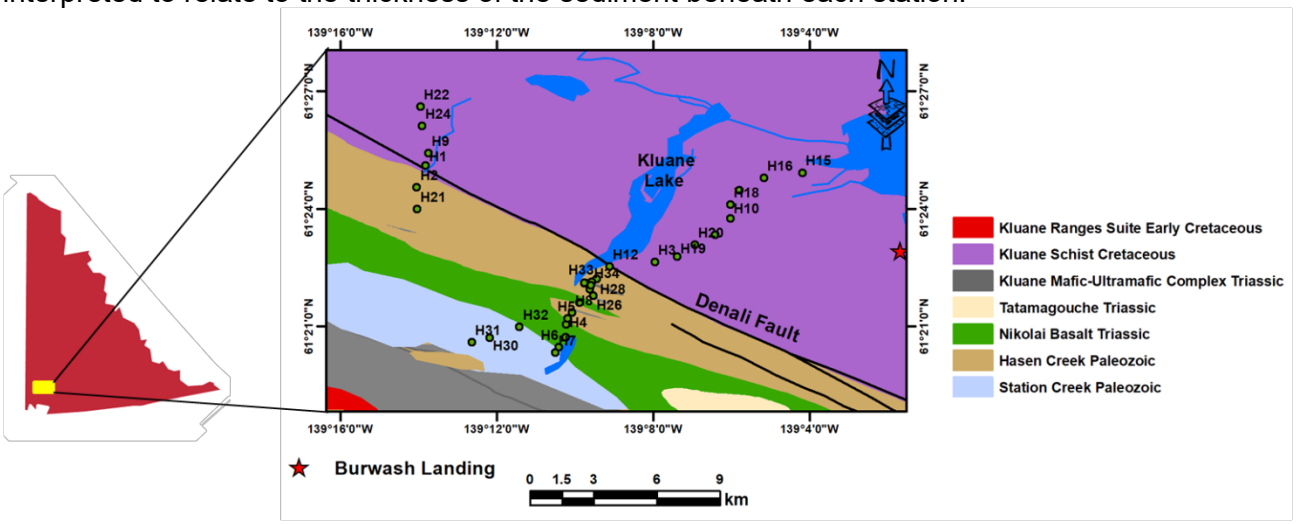


**Figure 1:** Geologic map of the Burwash Landing area (YGS, 2022). Denali Fault is shown as thick black lines. The study area is highlighted with yellow box in the map of Yukon Territory.

## HVSR Method

The widely used HVSR technique is a passive seismic monitoring approach that analyzes the ratio of horizontal to vertical (H/V) components (Köhler and Weidle, 2018; Berumen-Borrego et al., 2024) of ambient seismic noise, primarily from Rayleigh waves. The HVSR technique has recently become widely recognized for its applications in fault detection (Gosar, 2017; Khalili and Mirzakurdeh, 2019; Yulianto and Yuliyanto, 2023) and for mapping depth of contact between basement rocks and overlying sediments (Torrese et al., 2020; Mele et al., 2021; Berumen-Borrego et al., 2024).

Calculating HVSR curves of three-component seismic data involves determining the ratio of the spectra of the horizontal components to the vertical component. The primary signal in HVSR analysis is a spectral peak marking the resonance frequency ($f_0$) of a layer characterized by low seismic velocities. Determining the resonance frequency is essential for estimating the thickness of soft sedimentary layers (Kula et al., 2018), and it is sensitive to the shear wave velocity of the layer.

## Data Processing

The fundamental frequency, $f_0$, and amplification factor,$A_0$, for our study area were calculated using seismic data from 34 seismic sensors with design frequency of 5 Hz. The instruments recorded continuously in the summer of 2022. We processed data recorded by these instruments using the open-source analysis software HVSRPY (Cox et al., 2020). By calculating HVSR curves for each individual hour of recording; we can investigate temporal variations in the signal and explore potential factors that may contribute to these changes. For each hour of recording, the time series were divided into 100–second time windows. The 100-second window length was chosen based on finding it to provide stable and reliable HVSR curves, particularly at lower frequencies. Taken together; the series of separate HVSR curves for each hour of recording produces a spectrogram that exhibits how the resonant frequency varies with time. HVSR results were monitored across three months to investigate how conditions change from the late spring to the summer in the Yukon. Our analyses focus on portions of the spectral time series with little to no spurious changes in amplitude. This period of more stable recording occurs during August 2022.

## Results

The HVSR results across three months indicate variations in the amplitude and frequency of the resonant peak. Temporal variability in the resonant peak can result from factors such as changing environmental conditions (wind, precipitation, temperature etc.), and anthropogenic sources that affect the shallow subsurface. Comparing changes in HVSR signals to environmental conditions for Burwash Landing such as temperature, wind speed, and precipitation, we find that changes in HVSR appear to mirror changing environmental conditions.

As temperatures warm from the spring to summer in the Yukon, and the active layer within the uppermost shallow crust thaws, the trend in the resonant peaks in the HVSR curves to lower frequencies may result from these changing seasonal conditions (Figure 2). This gradual change in the resonant frequency may result from the seismic velocities of the shallow crust decreasing as the active layer melts and more water is present in the upper 5 m of the shallow crust (e.g., Köhler and Weidle, 2019; Cheng et al., 2022).

The HVSR curves calculated for the data recorded in August may be less affected by changing conditions in the active upper crust as they exhibit clear spectral peaks, and therefore, chosen and isolated for interpretation in this study. For the sensors recording near Burwash Landing, we find that their HVSR curves exhibit peaks within one of three distinct frequency ranges (0.3–4 Hz; 5–10 Hz and 11–20 Hz) (Figure 3).

The frequency of the spectral peaks relates to the thickness of sediments and depth to the basement in the location of the station. The pattern for the distribution of peak frequencies observed here adds to the trends observed by Berumen-Borrego et al., (2024), who investigated the area with a sparse array of broadband sensors and found HVSR curves with peaks at three distinct frequencies. In their work, Berumen-Borrego et al. (2024) observed HVSR curves with peaks as low as 0.3 Hz to the north of the Denali Fault that they modeled with a thick low velocity layer in which velocities increase following a power-law pattern to a depth of 300 m.

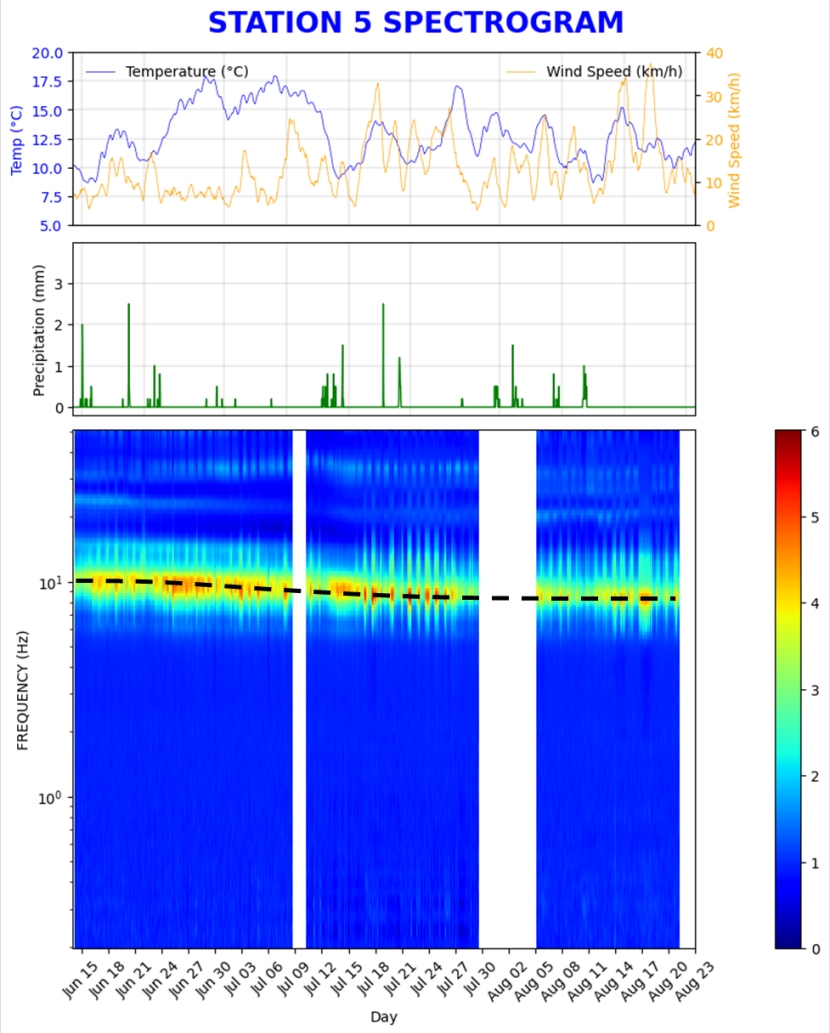


**Figure 2:** HVSR spectrogram for station 5. Dotted line follows the peak in the HVSR curves that vary from frequencies close to 10 Hz in June to ~8 Hz in August.

Berumen-Borrego et al. (2024) interpreted the base of the low velocity layer to indicate the boundary between thick sedimentary cover atop basement rock. To the south of the Denali Fault, they modeled HVSR curves with peak frequencies greater than 10 Hz with a layer extending to only 50 m indicating thin sedimentary cover. Closer to the Denali Fault, they fit HVSR curves with a peak between 7 and 8 Hz using a model comprised of a thinner low velocity layer extending to 170 m that marked the boundary between thick and thin sediment cover.

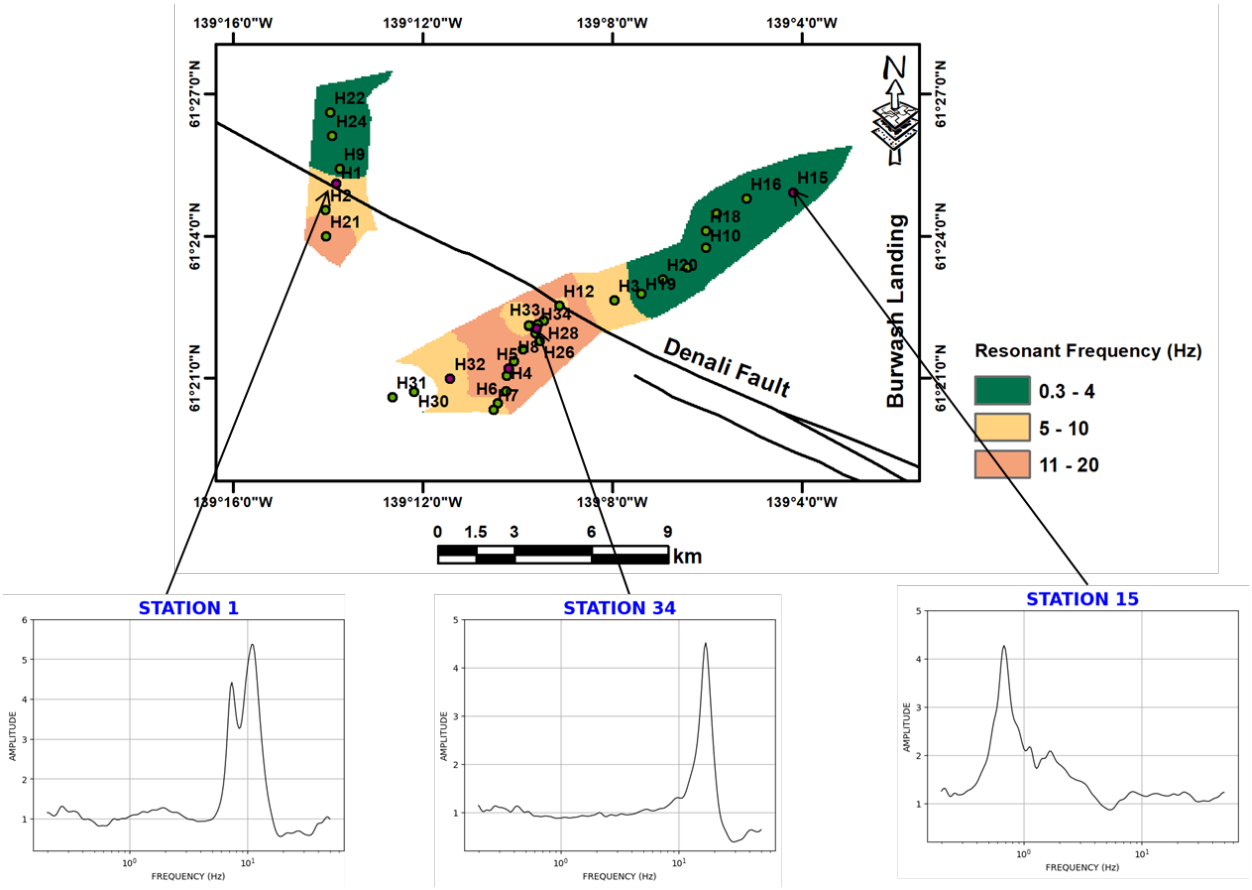


**Figure 3:** Map of the resonant frequency across the stations in the study area. HVSR curves for the month of August for some stations are also shown. Green dots represent sampling points of HVSR measurements while pink dots represent HVSR displayed results in this study.

Figure 3 shows HVSR curves with two distinct signatures separated by the Denali fault. Curves with a peak in the low frequency range between 0.3–4 Hz are observed to the north of the Denali fault, indicating a thick sediment unit overlying the basement. High frequency range between 10–20 Hz is observed to the south of the Denali fault, indicating thin sediment unit overlying the basement. Also, intermediate frequency range between 4–10 Hz is observed at the boundary of the Denali fault, indicating the transition zone between thin sediment layer and thick sediment layer. This observation was compared with Bouguer Anomaly from gravity observation detailed in Witter (2020) for the study area (Figure 4). Low Bouguer anomaly indicating the presence of lithologic unit with low density or deep-seated basement rocks correlates with low frequency range to the north of the Denali fault. In the same vein, high Bouguer anomaly indicating the presence of high-density lithologic unit or basement rocks with shallow depth to the top also correlate well with high frequency range in the south of the Denali fault. Stations 30 and 31 were omitted from further interpretation because the HVSR results cannot be relied on. The HVSR curves for these stations show spurious low frequency peaks that can be attributed to localized sources of noise.

Daily variability in amplitude of HVSR spectra are observed, with pronounced changes coinciding with periods of high precipitation and high wind speed. Accordingly, we focus our analysis on periods of low precipitation and low wind speed. These regions show subtle structures in the near surface highlighted by high frequency peaks as observed in stations 3, 5, 6, 7, 12, 14, 19 (highlighted in yellow in Figure 4). This correlate with ground observations from 2D resistivity model from electromagnetic measurement (Innovate Geothermal, 2020), highlighting the presence of subsurface structure interpreted as faults that could serve as pathways for the upwelling of geothermal heat and fluid to the surface (Figure 4). The correlation of these observations also showed that thick layer of Quaternary sediment overly the Kluane Schist. The result of this study highlights the application of seismic ambient noise in subsurface mapping in relation to mapping the depth to bedrock in an area of geothermal exploration by analyzing HVSR. Future endeavors will be focused on modelling HVSR observations to identify geologic structures present in this area by carrying out joint inversion of HVSVR results, magnetic and gravity data.

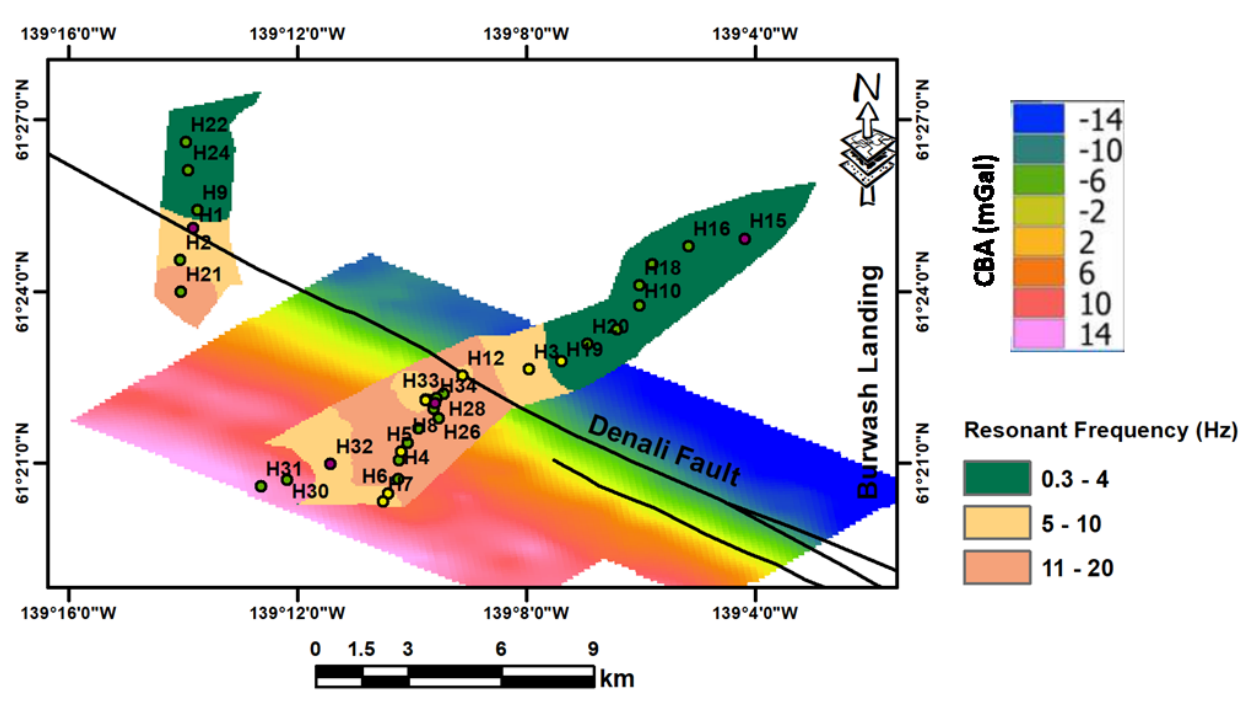


**Figure 4:** Map of the resonant frequency across the stations in the study area with overlay of the Bouguer anomaly map from Innovate Geothermal (2020). Green dots represent sampling points of HVSR measurements while pink dots represent HVSR displayed results in this study.

## Acknowledgements

We extend our gratitude to the Kluane First Nation for allowing us to conduct field measurements on their land. We also acknowledge the financial support from the University of Calgary, the Yukon Geological Survey, and from Natural Sciences and Engineering Research Council of Canada through Alliance Grant ALLRP-580887-22. The Natural Science and

Engineering Research Council of Canada further supports this work through Discovery grants awarded to Jan Dettmer and Hersh Gilbert, and a Postdoctoral Fellowship awarded to Jeremy M. Gosselin.

**References**

Balkan, E., Erkan, K. and Şalk, M. 2017. Thermal conductivity of major rock types in western and central Anatolia regions, Turkey. *Journal of Geophysics and Engineering* 14: 909–919.https://doi.org/10.1088/1742-2140/aa5831

Bender, A. and Haeussler, P. 2017. Eastern Denali Fault Surface Trace Map, Eastern Alaska and Yukon, Canada. U.S. Geological Survey, Open-File Report 2017–1049, 10 p., https://doi.org/10.3133/of20171049.

Berumen-Borrego, F., Gilbert, H., Dettmer, J., Gosselin, J.M. and Shahsavari P. 2024. Shearwave velocities from broadband HVSR measurements for geothermal resource assessment near Burwash Landing, Yukon. *In*: Yukon Exploration and Geology Technical Papers 2023, L.H. Weston and Purple Rock Inc. (eds.), Yukon Geological Survey, p. 1–15.

Chen, C. T., Kuo, C. H., Lin, C.-M., Huang, J. Y., Wen, K. L. 2022. Investigation ofshallow S-wave velocity structure and site response parameters in Taiwan by using high-density micro-tremor measurements. *Eng. Geol*. 297, 106498.https://doi.org/10.1016/j.enggeo.2021.106498.

Cheng, F., Xia, J., Ajo-Franklin, J. B., Behm, M., Zhou, C., Dai, T., et al. 2021. High-resolution ambient noise imaging of geothermal reservoir using 3C dense seismic nodal array and ultra-short observation. *Journal of Geophysical Research: Solid Earth*,*126*, e2021JB021827. https://doi.org/10.1029/2021JB021827

Cheng, F., Lindsey, N. J., Sobolevskaia, V., Dou, S., Freifeld, B., Wood, T., et al. 2022. Watching the cryosphere thaw: Seismic monitoring of permafrost degradation using distributed acoustic sensing during a controlled heating experiment. *Geophysical Research Letters*, *49*, e2021GL097195.https://doi.org/10.1029/2021GL097195.

Cox, B.R., Cheng, T., Vantassel, J.P. & Manuel, L., 2020. A statistical representationand frequency-domain window-rejection algorithm for single station HVSR measurements. *Geophys. J. Int.,* 221, 2170–2183. https://doi.org/10.1093/gji/ggaa119.

Elbshbeshi, A., Gomaa, A., Mohamed, A., Othman, A., Ghazala, H. 2022. Seismic hazard evaluation by employing microtremor measurements for Abu Simbel area, Aswan, Egypt. *J. Afr. Earth Sci.* 196, 104734 https://doi.org/10.1016/j.jafrearsci.2022.104734.

Fat-Helbary, R.E.S., El-Faragawy, K.O., Hamed, A. 2019. Application of HVSR technique in the site effects estimation at the south of Marsa Alam city, Egypt. *J. Afr. Earth Sci.* 154, 89–100. https://doi.org/10.1016/j.jafrearsci.2019.03.015.

Faulds, J.F. & Hinz, N.H. 2015. Favorable tectonic and structural settings of geothermal systems in the Great Basin Region, Western USA: Proxies for discovering blind geothermal systems. Proceedings World Geothermal Congress, Melbourne, Australia, 19–25 April 2015, 6 p.

Fraser, T.A., Grasby, S.E., Witter, J.B., Colpron, M. & Relf, C. 2018. Geothermal studies in Yukon–collaborative efforts to understand ground temperature in the Canadian North. GRC Transactions, vol. 42, 20 p.

Global Volcanism Program 2013. Volcanoes of the World, v. 4.8.4. Venzke, E (ed.). Smithsonian Institution. <http://volcano.si.edu/> [accessed January 24, 2025].

Gosar, A. 2010. Site effects and soil-structure resonance study in the Kobarid basin (NW Slovenia) using microtremors. Nat. *Hazards Earth Syst. Sci.* 10. https://doi.org/10.5194/nhess-10-761-2010.

Innovate Geothermal, 2020. Early–stage exploration for geothermal energy resources along the Denali fault near Duke River, Yukon. Unpublished technical report prepared by Innovate Geothermal for the Yukon Geological Survey, 94p

Kämmelein, M., Diet, C. & Stollhofen, H. 2019. The Franconian basin thermal anomaly: testing its origin by conceptual 2-D models of deep-seated heat sources covered by low thermal conductivity sediments. *International Journal of Energy and Environmental Engineering* 10: 389–412. https://doi.org/10.1007/s40095-019-00315-2

Khalili, M. and Mirzakurdeh, A. V. 2019. Fault detection using microtremor data (HVSR–based approach) and electrical resistivity survey. *Journal of Rock Mechanics and Geotechnical Engineering* 11. 400–408. https://doi.org/10.1016/j.jrmge.2018.12.003.

Köhler, A. and Weidle, C. 2019. Potentials and pitfalls of permafrost active layer monitoring using the HVSR method: a case study in Svalbard. *Earth Surf. Dynam.,* 7, 1–16. https://doi.org/10.5194/esurf-7-1-2019.

Konno, K., Ohmachi, T. 1998. Ground-motion characteristics estimated from spectral ratio between horizontal and vertical components of microtremor. *Bull. Seismol. Soc. Am.* 88, 228–241. https://doi.org/10.1785/BSSA0880010228.

Koteas, C. G., Rhodes, J. M., Mabee, S. B., Goodhue, N. and Adams, S. A. 2011. Identifying and examining potential geothermal resources in non-traditional regions, examples from the northeastern U.S. *Abstracts with Programs - Geological Society of America* 43, 40–40.

Kula, D., Olszewska, D., Dobiński, W. and Glazer, M. 2018. Horizontal–to vertical spectral ratio variability in the presence of permafrost. *Geophysical Journal International* 214, 219–231. https://doi.org/10.1093/gji/ggy118.

Li, C.F., Lu, Y., Wang, J. 2017. A global reference model of Curie-point depths based on EMAG2. Nature, Scientific Reports, v. 7 https://doi.10.1038/srep45129. 9 p.

Mahmood, K., Zamin, B., Iqbal, S., Zia-Ur-Rehman, Afzal, S., Safdar, M., Iqbal, Q., Ali, A. 2022. Local site effect on seismic hazard of the relocated new Balakot town. SoilDynam. Earthq. Eng. 162, 107451 https://doi.org/10.1016/j.soildyn.2022.107451.

Mele, M., Bersezio, R., Bini, A., Bruno, M., Giudici, M. and Tantardini, D. 2021. Subsurface profiling of buried valleys in central alps (northern Italy) using HVSR single–station passive seismic. *Journal of Applied Geophysics* 193. 104407. https://doi.org/10.1016/j.jappgeo.2021.104407.

Nakamura, Y. 1989. A method for dynamic characteristics estimation of subsurface using microtremor on the ground surface. *Railway Technical Research Institute, Quarterly Reports*, *30*(1). https://trid.trb.org/view/294184.

Russell, J.K., Edwards, B.R., Williams-Jones, G. and Hickson, C.J. 2023. Pleistocene to Holocene volcanism in the Canadian Cordillera. *Canadian Journal of Earth Sciences*. 60 (10): 1443-1466. https://doi.org/10.1139/cjes-2023-0065

Torrese, P., Rossi, A. P., Unnithan, V., Pozzobon, R., Borrmann, D., Lauterbach, H., Luzzi, E. and Sauro, F. 2020. HVSR passive seismic stratigraphy for the investigation of planetary volcanic analogues. *Icarus* 351 (113970). https://doi.org/10.1016/j.icarus.2020.113970.

Witter, J. B., Miller, C. A., Friend, M., Colpron, M. 2018. Curie point depths and heat production in Yukon, Canada *Proceedings, 43rd Workshop on Geothermal Reservoir Engineering Stanford University, Stanford, California, February 12-14, 2018* SGP-TR-213.

Witter, J. B. 2020. Early-stage exploration for geothermal energy resources along the Denali fault near Duke River, Yukon. *Yukon Geological Survey, Open File 2020-3.* https://data.geology.gov.yk.ca/Reference/95836#InfoTab.

Yuliyanto, G. and Yulianto, T. 2023. Microtremor data and HVSR method of geothermal manifestation of Mt. Telomoyo, Central Java, Indonesia. *Data in Brief* 51 (109721). https://doi.org/10.1016/j.dib.2023.109721.

Yukon Geological Survey. 2022. Yukon digital bedrock geology. *Yukon Geological Survey*, https://data.geology.gov.yk.ca/Compilation/3. [accessed January12, 2024].